Eur. Phys. J. C 22, 411–421 (2001)
Digital Object Identifier (DOI) 10.1007/s100520100817

THE EUROPEAN PHYSICAL JOURNAL C

$\mathcal{CP}$ odd anomalous interactions of Higgs boson in its production at photon colliders

I.F. Ginzburg[1,2,a], I.P. Ivanov[1,2,3,b]

[1] Institute of Mathematics, Novosibirsk, Russia
[2] Novosibirsk State University Novosibirsk, Russia
[3] IKP, Forschungszentrum Jülich, 52405 Jülich, Germany

Received: 22 January 2001 /
Published online: 23 November 2001 –

Abstract. We discuss the potentialities of the study of $\mathcal{CP}$ odd interactions of the Higgs boson with photons via its production at $\gamma\gamma$ and $e\gamma$ colliders. Our treatment of $H\gamma\gamma$ and $HZ\gamma$ anomalous interactions includes a set of free parameters, whose impact on physical observables has not been considered before. We focus on two reactions, $\gamma\gamma \to H$ and $e\gamma \to eH$, and introduce the polarization and/or azimuthal asymmetries that are particularly sensitive to specific features of the anomalies. We discuss the ways of disentangling the effects of physically different parameters of the anomalies and estimate what the magnitude of $\mathcal{CP}$ violating phenomena is that can be seen in these experiments.

1 Introduction

In [1] we studied possibilities to discover $\mathcal{CP}$ even anomalous interactions of the Higgs boson via its production at $\gamma\gamma$ and γe colliders. Below we analyze the effects of $\mathcal{CP}$-parity violating anomalies. These result in the polarization and azimuthal asymmetries in the Higgs boson production. With new opportunities for the variation of the photon polarization at photon colliders [2], the Higgs boson production at $\gamma\gamma$ and γe colliders has an exceptional potential in the extraction of these anomalies. To some extent, some similar issues have been considered in [3–8]. However, in the analysis in these references the polarization potential was not used in its complete form and some natural degrees of freedom in the parameter space were not considered. Besides, the authors cited consider either $\gamma\gamma$ or γe collisions separately. In the present paper we have in mind that experiments in $\gamma\gamma$ and γe collider modes will supplement each other and provide complementary opportunities in investigating Higgs boson anomalous interactions.

In our analysis we assume the Higgs boson to be discovered by the time the Photon Collider starts operating, so that its basic properties will be known by that time. For definiteness, we assume that the Higgs boson coupling constants will be found experimentally to lie close to their SM values. Our idea essentially is that it is necessary to make use of a step-by-step strategy in studying anomalous effects. Namely, the first step is the study of $H\gamma\gamma$ anomalies in $\gamma\gamma$ collisions and the second step is using γe collisions for the study of $HZ\gamma$ anomalies assuming $H\gamma\gamma$ anomalies (both $\mathcal{CP}$ even and $\mathcal{CP}$ odd) to be studied at the first stage (with higher accuracy than it is possible at the second stage).

The $\gamma\gamma$ and γe colliders will be the specific modes of the future linear colliders (in addition to the e^+e^- mode) with the following typical parameters [9,10] (E and $\mathcal{L}_{ee}$ are the electron energy and luminosity of the basic e^+e^- collider).

(1) Characteristic photon energy $E_\gamma \approx 0.8E$.
(2) Annual luminosity is typically $\mathcal{L}_{\gamma\gamma} \approx 200\,\mathrm{fb}^{-1}$.
(3) Mean energy spread $\langle \Delta E_\gamma \rangle \approx 0.07 E_\gamma$.
(4) Mean photon helicity $\langle \lambda_\gamma \rangle \approx 0.95$ with variable sign [9].
(5) Circular polarization of the photons can be transformed into the linear one [9,2].

The effective photon spectra for these colliders are given in [11]. With the above properties, considering photon beams at the Photon Collider as roughly monochromatic is a good approximation for our purposes.

The value of effects which can be observed in experiment is given by the expected accuracy in the measuring of the cross sections under interest. For the $\gamma\gamma$ colliders the expected accuracy in measuring of the Higgs boson decay width will be 2% or better [12]. For the $e\gamma \to eH$ process we assume the achievable accuracy to be $5 \div 10\%$.

Throughout this paper we denote by λ and $\zeta/2$ the average helicities of photons and electrons and by ℓ the average degree of the photon linear polarization. We use some SM notation: $s_\mathrm{W} = \sin\theta_\mathrm{W}$, $c_\mathrm{W} = \cos\theta_\mathrm{W}$, $v_e = 1 - 4\sin^2\theta_\mathrm{W}$ and $v = 246\,\mathrm{GeV}$ (Higgs field v.e.v.). In the numerical calculations we assume the Higgs boson to lie

[a] e-mail: ginzburg@math.nsc.ru
[b] e-mail: i.ivanov@fz-juelich.de

in the most expected mass interval 110–250 GeV. Some further notation is borrowed from [1].

2 Sources of $\mathcal{CP}$ violation. Parameterization

We consider below triple Higgs boson anomalous interactions $H\gamma\gamma$ and $HZ\gamma$ in the processes $\gamma\gamma \to H$ and $\gamma e \to eH$. The quartic interactions lie beyond our scope.

One can imagine two possible mechanisms of $\mathcal{CP}$ violation in the interactions of the Higgs boson. First, the observed Higgs boson can be a mixture of purely scalar and pseudoscalar fields, as can happen in the multi-doublet Higgs models or in MSSM; see for details e.g. [3,13] and Sect. 5 as an example. In this case $\mathcal{CP}$ violating effects could be either weak or strong.

The second possibility is that the Higgs boson itself is $\mathcal{CP}$ even fundamentally, but underlying interactions can break the $\mathcal{CP}$ parity conservation law. In this case we expect small $\mathcal{CP}$ violating effects in the interactions of the Higgs boson with the known particles. In turn, this type of $\mathcal{CP}$ violation can be caused either by the effects in the underlying theory, similar to the aforementioned mixing, or by fundamental effects related, for example, to the breaking of unitarity of the S-matrix at very small distances. (In the latter case the $\mathcal{CP}$ breaking can originate, in principle, from the possibility that the S-matrix is unitary only when written in terms of *observable asymptotic states* and the unitarity appears broken if the space of states is expanded by adding the *unobservable* unstable H final states.)

A natural question then arises, namely, whether we can distinguish between these two possible causes of $\mathcal{CP}$ violation: i.e. *whether the energy scale of $\mathcal{CP}$ violation Λ is low or high.* In order to answer this question, one should study how corresponding amplitudes depend on additional kinematical variables, such as the total energy $s^{1/2}$, photon virtualities Q^2 etc., i.e. on Q^2/Λ^2, s/Λ^2, etc. Indeed, in the first case the dependence on these parameters could be observable, while in the second case the above dimensionless parameters are small and the corresponding amplitudes appear to be independent from these kinematical variables. (The latter case is described usually with the aid of effective Lagrangians.) However, a specific feature of the reaction $\gamma\gamma \to H$ is that its kinematics is fixed. This makes it impossible to observe any additional dependence on Λ. As we turn to the process $e\gamma \to eH$, one kinematical degree of freedom appears, namely, the virtuality Q^2 of the exchanged photon or Z. However, as shown in [1], the bulk of the cross section comes from the region $Q^2/M_H^2 \ll 1$, which again leaves us unable to learn about the source of $\mathcal{CP}$ violation.

The outcome of this discussion can be summarized as follows: when considering real Higgs boson production in the two processes discussed, the above two sources of $\mathcal{CP}$ violation are indistinguishable in the discussed experiments.

Given this, we follow the natural procedure to describe the deviation of discussed production amplitudes from their SM values in a universal manner. We parameterize the $H\gamma\gamma$ and $HZ\gamma$ amplitudes (which will be also referred to as effective $H\gamma\gamma$ and $HZ\gamma$ vertices) in the operator form, similar to that for the effective Lagrangian:

$$\mathcal{M}_{\gamma\gamma H} = \frac{1}{v}\left[G_\gamma H F^{\mu\nu}F_{\mu\nu} + \mathrm{i}\tilde{G}_\gamma H F^{\mu\nu}\tilde{F}_{\mu\nu}\right],$$
$$\mathcal{M}_{\gamma Z H} = \frac{1}{v}\left[G_Z H Z^{\mu\nu}F_{\mu\nu} + \mathrm{i}\tilde{G}_Z H Z^{\mu\nu}\tilde{F}_{\mu\nu}\right]. \quad (1)$$

Here $F^{\mu\nu}$ and $Z^{\mu\nu}$ are the standard field strengths for the electromagnetic and Z field and $\tilde{F}^{\mu\nu} = \varepsilon^{\mu\nu\alpha\beta}F_{\alpha\beta}/2$. The dimensionless parameters G_i are effective coupling constants. They are sums of the well-known SM contributions (see e.g. [1] for the normalization)[1] and anomalous parts g_i ("anomalies"), describing the strength of the interactions beyond SM, which are generally complex:

$$G_i = G_i^{\mathrm{SM}} + g_i, \quad \tilde{G}_i = g_{Pi}, \quad g_a = |g_a|\mathrm{e}^{\mathrm{i}\xi_a}. \quad (2)$$

The complex values of the "couplings" g_a are quite natural. Indeed, recall that even G_i^{SM} are complex due to contributions, for example, of the b quark loop in the amplitude. The same is valid in various versions of the first variant of $\mathcal{CP}$ violation. One particular example of this is discussed in Sect. 5, where the anomaly can be defined simply as the difference between the minimal SM and two doublet Higgs model (II) with $\mathcal{CP}$ violation. If $\tan\beta \gg 1$, the contribution of the b quarks in loops is enhanced, which gives rise to the large imaginary part of the amplitudes. For the second mechanism a complex g_i could be the signal of fundamental breaking of the unitarity in the theory.

We assume that future observations will reveal a picture close to SM and therefore the anomalies g_i will be small. In the first mechanism of $\mathcal{CP}$ violation with $\Lambda \lesssim M_H$ the smallness of the anomalies is related to small values of the corresponding mixing angles α_m, $g_i \sim \alpha_m$. In the second mechanism it is related to the large scale of new physics Λ, i.e. $g_i = (v/\Lambda_i)^2$ with $\Lambda_i \sim \Lambda$. The relation between the parameters Λ_i and Λ depends on the nature of new physics.

(A) The simplest extension of the SM consists in adding new charged heavy particles with mass M_n not generated by a Higgs mechanism (like in MSSM). They will circulate in loops and give rise to anomalous effective $H\gamma\gamma$ and $HZ\gamma$ vertices, with $\Lambda^2 \sim 4\pi M_n^2/\alpha$.
(B) If the heavy particle is a point-like Dirac monopole, then $\Lambda^2 \sim \alpha M_n^2$.
(C) If the new physics is determined by a higher dimension (Kaluza–Klein) mechanism, the quantity Λ is close to the energy scale at which the extra dimensions come into play.

For the second mechanism the anomalous amplitude is often described with the aid of an effective Lagrangian with operators of dimension 6, which has the same form as our effective vertices (1). Our particular parameterization can be readily linked to that used in other papers (e.g. [6,15,16]). For example, the correspondence of

[1] With the proposed experimental accuracy, when doing the final numerical calculation, one should, of course, use $H\gamma\gamma$ coupling with radiative corrections [14]

our parameters g_i to the constants d_i used in [6] reads $d_{Z\gamma} = 2g_{Z\gamma}/(c_{\rm W}s_{\rm W})$, $\bar{d}_{Z\gamma} = g_{PZ}/(c_{\rm W}s_{\rm W})$.

Finally, we undertake a study where both $|g_i|$ and ξ_i are treated as *independent parameters*. This is done in contrast to other, similar investigations, where the complexity was not an explicitly free parameter, but fixed by the particular model considered. We argue that our approach accounts for the widest range of possible anomalies. Determination of both sets of parameters should be considered primarily as an experimental task[2].

About figures and notation

Currently, due to the large number of new model parameters, a thorough investigation of the regions of the parameter space achievable in future experiments makes little sense. Instead of that we present in our figures examples for some values of parameters, which illustrate that the study of these effects at the photon colliders is indeed possible and profitable.

There are no doubts that relatively large anomalies will be discovered easily. Therefore, we concentrate our efforts on the case when the anomalous effects are relatively small as compared with basic SM effects. In this case the effects of anomalies will be seen mainly in the interference with the SM effects, and contributions of different anomalies in the observed cross sections are additive to a good accuracy. This is why we treat each anomaly separately, assuming all other anomalies absent (the corresponding $g_i = 0$).

3 Process $\gamma\gamma \to H$

Let us denote by $\langle\sigma^{\rm SM}\rangle_{\rm np}$ the SM Higgs boson production cross section in unpolarized photon collisions averaged over a certain small effective mass interval (see e.g. [1]). Then the cross section of the Higgs boson production can be written in the form

$$\begin{aligned}
&\langle\sigma\rangle(\lambda_i,\ell_i,\psi) = \langle\sigma^{\rm SM}\rangle_{\rm np} T(\lambda_i,\ell_i,\psi),\\
&T(\lambda_i,\ell_i,\psi) = \frac{|G_\gamma|^2}{|G_\gamma^{\rm SM}|^2}(1+\lambda_1\lambda_2+\ell_1\ell_2\cos 2\psi)\\
&\quad+\frac{|\tilde G_\gamma|^2}{|G_\gamma^{\rm SM}|^2}(1+\lambda_1\lambda_2-\ell_1\ell_2\cos 2\psi)\\
&\quad+2\frac{{\rm Re}(G_\gamma^*\tilde G_\gamma)}{|G_\gamma^{\rm SM}|^2}(\lambda_1+\lambda_2)+2\frac{{\rm Im}(G_\gamma^*\tilde G_\gamma)}{|G_\gamma^{\rm SM}|^2}\ell_1\ell_2\sin 2\psi.
\end{aligned}\tag{3}$$

Here λ_i and ℓ_i $(i = 1, 2)$ are the degrees of the circular and linear polarization respectively of the photon beams, and ψ is the polar angle between the linear polarization vectors of the two photon beams.

In the SM case we have only the first item in this sum. (Note that the $\gamma\gamma \to b\bar b$ background is practically independent on the linear polarization of the photons.)

An important feature here is the interference terms. They give rise to the inequality of the two directions of rotation and to the modification of the ψ dependence, which is entirely due to the $\mathcal{CP}$ odd admixture to the $\mathcal{CP}$ even Lagrangian. Owing to these modifications, a number of experimentally measurable quantities appear that can help study the $\mathcal{CP}$ even and odd anomalies separately.

It is useful to introduce five different asymmetries:

$$\begin{aligned}
T_\pm &= \frac{\langle\sigma\rangle(\lambda_i,\ell_i=0)\pm\langle\sigma\rangle(-\lambda_i,\ell_i=0)}{2\langle\sigma^{\rm SM}\rangle_{\rm np}}\\
&\propto\begin{cases}(1+\lambda_1\lambda_2)(|\tilde G_\gamma|^2+|G_\gamma|^2),\\ 2(\lambda_1+\lambda_2){\rm Re}(\tilde G_\gamma^* G_\gamma);\end{cases}\\
T_\parallel &= \frac{\langle\sigma\rangle(\lambda_i=0,\ell_i,\psi=0)}{\langle\sigma^{\rm SM}\rangle_{\rm np}}\\
&\propto\left[|G_\gamma|^2(1+\ell_1\ell_2)+|\tilde G_\gamma|^2(1-\ell_1\ell_2)\right],\\
T_\perp &= \frac{\langle\sigma\rangle(\lambda_i=0,\ell_i,\psi=\pi/2)}{\langle\sigma^{\rm SM}\rangle_{\rm np}}\\
&\propto\left[|G_\gamma|^2(1-\ell_1\ell_2)+|\tilde G_\gamma|^2(1+\ell_1\ell_2)\right],\\
T_\psi &= \frac{\langle\sigma\rangle(\lambda_i=0,\ell_i,\psi=3\pi/4)-\langle\sigma\rangle(\lambda_i=0,\ell_i,\psi=\pi/4)}{\langle\sigma^{\rm SM}\rangle_{\rm np}}\\
&\propto 2\ell_1\ell_2{\rm Im}(\tilde G_\gamma^* G_\gamma),
\end{aligned}\tag{4}$$

whose SM values are

$$\begin{aligned}
&T_+^{\rm SM} = 1+\lambda_1\lambda_2, \quad T_-^{\rm SM} = 0,\\
&T_\parallel^{\rm SM} = 1+\ell_1\ell_2, \quad T_\perp^{\rm SM} = 1-\ell_1\ell_2, \quad T_\psi^{\rm SM} = 0.
\end{aligned}$$

The quantities T_+, $T_\parallel$ and $T_\perp$ are combinations of $|G_\gamma|^2$ and $|\tilde G_\gamma|^2$ with different weights. These asymmetries are sensitive to the $\mathcal{CP}$ even anomaly and its phase ξ_γ via its interference with the SM contribution. The best quantity for this study is of course T_+, which is illustrated by Fig. 1. Certainly, curves for $\mathcal{CP}$ even anomaly effects at $\xi_\gamma = 0$ are the same as obtained in [1] (modulo reparameterization of anomalous terms). These three quantities include also the $\mathcal{CP}$ odd anomaly in the form $|\tilde G_\gamma|^2$, which is $\sim g_{P\gamma}^2$, i.e. small and independent of $\xi_{P\gamma}$ (the corresponding $g_{P\gamma}$ dependence was studied in [5]). Even in the case of $T_\perp$, where the contribution of $|\tilde G_\gamma|^2$ is enhanced, it is difficult to see the effect of $\mathcal{CP}$ odd anomalies at reasonably small $g_{P\gamma}$; see Fig. 3.

The remaining two quantities – T_- and T_ψ – are much more useful for a study of $\mathcal{CP}$ violating effects in the $\gamma\gamma H$ interaction. Their studies supplement each other. Both differ from zero only if the $\mathcal{CP}$ parity is broken. They derive from the interference of the $\mathcal{CP}$ odd and $\mathcal{CP}$ even items in (1). Figure 2 shows the T_- dependence on $|g_{P\gamma}|$ and the phase $\xi_{P\gamma}$ for different values of the Higgs boson mass.

[2] Certainly, only phase differences are measurable for entire effective couplings. Expecting a relatively small magnitude of the anomaly, one can conclude that the phases of the entire quantities G_γ, G_Z are close to their SM values $\xi_\gamma^{\rm SM}$ and $\xi_Z^{\rm SM}$ and the effect of the anomaly itself is reduced by a factor $\cos(\xi_\gamma - \xi_\gamma^{\rm SM})$

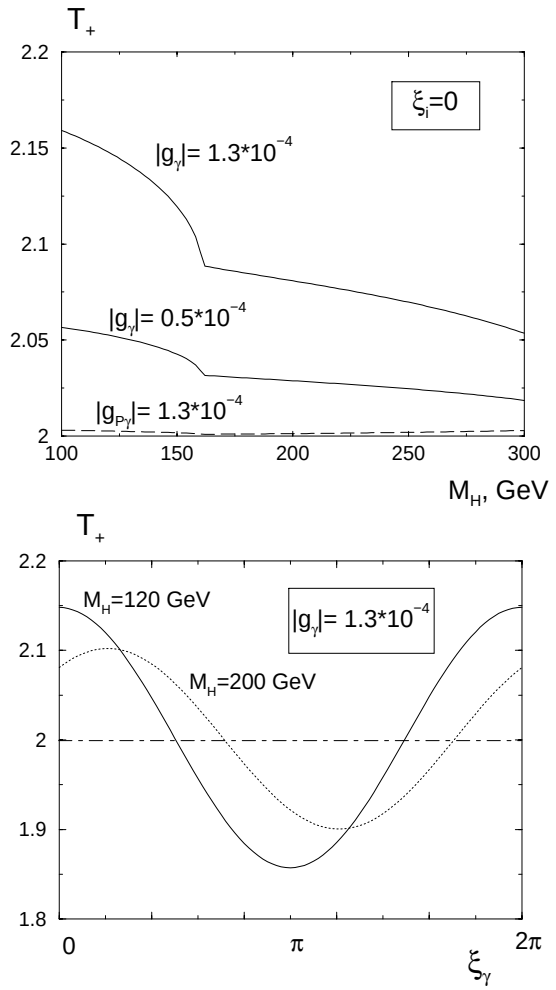

Fig. 1. The quantity T_+; $\lambda_1\lambda_2 = 1$

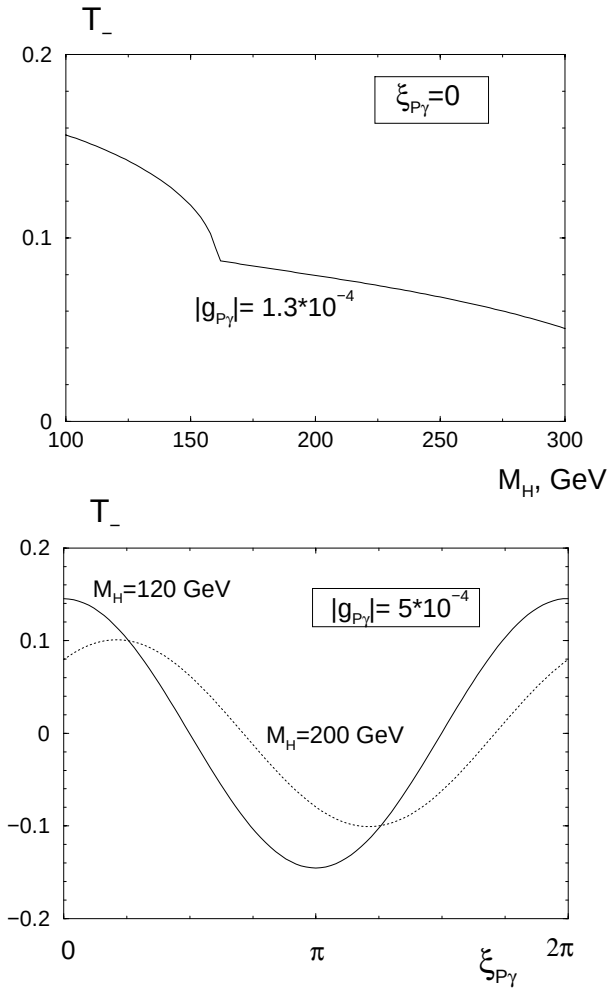

Fig. 2. The quantity T_-; $\lambda_1\lambda_2 = 1$

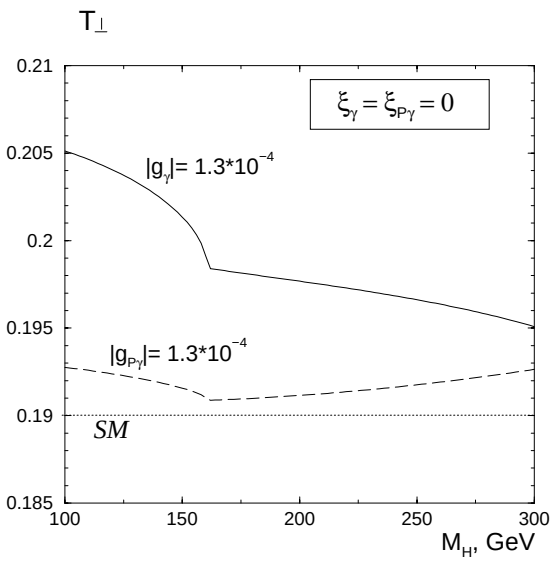

Fig. 3. The quantity $T_\perp$; $\ell_i = 0.9$

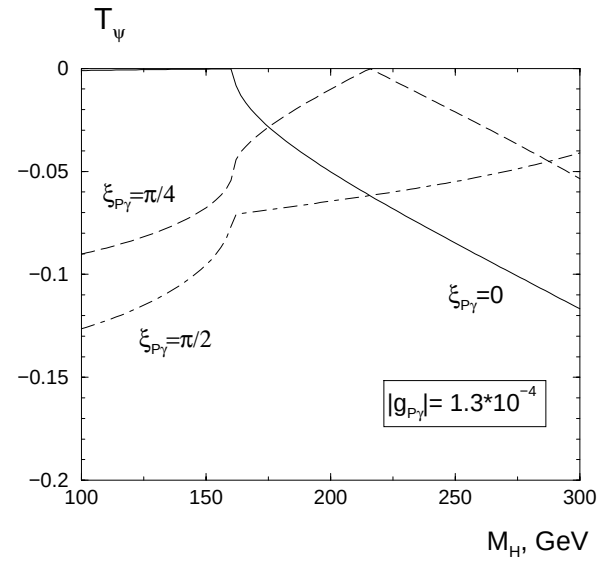

Fig. 4. The quantity T_ψ; $\ell_i = 0.9$

At $M_H < 160\,\mathrm{GeV}$ (WW threshold) the basic quantity G_γ^{SM} is practically real. Therefore, the quantity T_- has a maximum at $\xi_{P\gamma} = 0$. Above this threshold the imaginary part of G_γ^{SM} becomes substantial, and the position of the maximum is shifted to $\xi_{P\gamma} \neq 0$. Figure 4 shows that the $\mathcal{CP}$ odd anomaly effect is strong in this asymmetry as well, and exhibits a remarkable dependence of T_ψ on the value of the phase $\xi_{P\gamma}$. With a measurement of T_- and T_ψ one can extract from the data both $|g_{P\gamma}|$ and $\xi_{P\gamma}$ since T_- and T_ψ represent the real and imaginary part of the same quantity.

4 Process $e\gamma \to eH$

The process $e\gamma \to eH$ is considered here as a good tool for the study of the $HZ\gamma$ anomalous interactions provided the $H\gamma\gamma$ anomalies are known from the experiments in the $\gamma\gamma$ mode. This process was studied within SM in detail in [1,17][3]. It is described by diagrams of three types – those with photon exchange in the t-channel, with Z exchange in the t-channel and box diagrams. This subdivision is approximately gauge invariant with accuracy $\sim m_e/M_Z$ [1]. The difference in the cross sections σ^{L} and σ^{R} for the left-handed and right-handed polarized electrons is due to interference between photon and Z exchange amplitudes.

The main contribution to the total cross section is given by diagrams with photon exchange in the t-channel. Therefore, this total cross section is sensitive to the $H\gamma\gamma$ anomalies and weakly sensitive to the $HZ\gamma$ anomalies, which are our major concern here (the difference $\sigma^{\mathrm{L}} - \sigma^{\mathrm{R}}$ is small as compared with the unpolarized cross section). This picture is improved with the growth of the transverse momentum of the scattered electron $p_\perp$. Indeed, when this growth occurs, the photon exchange contribution is strongly reduced, while the Z boson exchange contribution changes only marginally at $p_\perp \lesssim M_Z$. At transverse momenta of the scattered electrons $p_\perp > 30\,\mathrm{GeV}$ and for longitudinally polarized initial electrons the effect of Z exchange should be seen well [1]. To feel the scale of the observed effects, we present in Fig. 5 the SM cross sections σ^{L} and σ^{R} integrated over the region $Q^2 > 1000\,\mathrm{GeV}^2$ and averaged over initial photon polarizations. We use this limitation in Q^2 everywhere below.

We denote the particle momenta p for the incident electron, k for the photon, $p' = p - q$ for the scattered electron and $Q^2 = -q^2$. In our calculations far from the photon pole in the t-channel we neglect the electron mass. We also denote $u = 2kp' = M_H^2 + Q^2 - s$, $x = 2kq/s \equiv (M_H^2 + Q^2)/s$, $E_{\mathrm{tot}} = s^{1/2}$. The collision axis is labeled the z axis, and the x axis is chosen along the direction of the photon linear polarization vector $\boldsymbol{\ell}$. Finally, the angle ϕ is the azimuthal angle of the scattered electron relative to the x axis so defined. The values $\zeta = -1$ or $\zeta = +1$ correspond to left-handed or right-handed polarized initial

[3] The production of the pseudoscalar Higgs boson in such a reaction was studied e.g. in [18]; see also [19] for the MSSM case

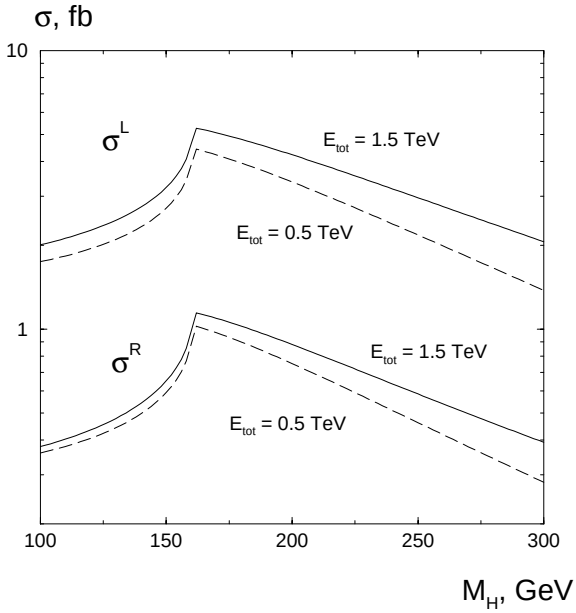

Fig. 5. The SM cross section of the $e\gamma \to eH$ process, $Q^2 > 1000\,\mathrm{GeV}^2$

electrons. We use superscripts L and R to label quantities referring to these polarizations.

The qualitative features of the observable effect could be understood taking into account that the quantities below could be treated as the average helicity λ_V and degree of linear polarization ℓ_V of an exchanged virtual photon or Z boson:

$$\lambda_V = \frac{s^2 - u^2}{s^2 + u^2}\zeta = \frac{x - x^2/2}{1 - x + x^2/2}\zeta,$$
$$\ell_V = \frac{2s|u|}{s^2 + u^2} = \frac{1 - x}{1 - x + x^2/2}, \qquad (5)$$

with the vector of the linear polarization $\boldsymbol{\ell}_V$ lying in the electron scattering plane [20]. Since usually $x \ll 1$, we have $\lambda_V \ll 1$ and $\ell_V \approx 1$. Therefore, joining the results of the previous section and those from [1], one can conclude that the effect of the $\mathcal{CP}$ odd $HZ\gamma$ interaction can be seen in the dependence on the angle ϕ in the experiments with left- and right-polarized electrons and in the study of the dependence on the sign of the incident photon helicity. These dependences have not been studied earlier.

The helicity amplitudes of the process are calculated just as in [1]. With the notations for the box contributions from that paper we have (in these equations the helicities $\lambda, \zeta = \pm 1$)

$$\mathcal{M} = -\frac{4\pi\alpha}{M_W s_{\mathrm{W}}}\sqrt{\frac{Q^2}{2}}\left\{s\frac{1+\zeta\lambda}{2} + (s - M_H^2 - Q^2)\right.$$
$$\left.\times\left[\frac{1-\zeta\lambda}{2}\cos 2\phi + \frac{\zeta-\lambda}{2}\mathrm{i}\sin 2\phi\right]\right\}(\lambda K + \tilde{K})$$
$$\left(K = V - \zeta A + B_+, \quad \tilde{K} = \tilde{V} - \zeta\tilde{A} + \zeta B_-\right). \qquad (6)$$

Here V and A stand for vector and axial t-channel exchange contributions, $B_\pm$ are the box contributions which

are composed from items related to the W or Z circulating in the box[4]:

$$
\begin{aligned}
V &= \frac{G_\gamma}{Q^2} + \frac{v_e G_Z}{4 s_\mathrm{W} c_\mathrm{W} (Q^2 + M_Z^2)},\\
A &= -\frac{G_Z}{4 s_\mathrm{W} c_\mathrm{W} (Q^2 + M_Z^2)},\\
\tilde{V} &= \frac{\tilde{G}_\gamma}{Q^2} + \frac{v_e \tilde{G}_Z}{4 s_\mathrm{W} c_\mathrm{W} (Q^2 + M_Z^2)},\\
\tilde{A} &= -\frac{\tilde{G}_Z}{4 s_\mathrm{W} c_\mathrm{W} (Q^2 + M_Z^2)},\\
B_\pm &= \frac{\alpha M_W^2}{4\pi s_\mathrm{W}^2}\\
&\quad \times \left[\frac{W(s,u) \pm W(u,s)}{2} + \frac{Z(s,u) \pm Z(u,s)}{2}\right]. \qquad (7)
\end{aligned}
$$

The amplitude squared for an arbitrarily polarized photon beam can be written in terms of the helicity amplitudes and the photon density matrix ρ written in a helicity basis as

$$
\begin{aligned}
|\mathcal{M}|^2 &= \mathcal{M}^*_a \rho_{a\,b} \mathcal{M}_b, \quad a,b = +,-,\\
\rho &= \frac{1}{2}\begin{pmatrix} 1+\lambda & -\ell \\ -\ell & 1-\lambda \end{pmatrix}. \qquad (8)
\end{aligned}
$$

Therefore, the cross section reads (here $\zeta = \pm 1$)

$$
\begin{aligned}
\mathrm{d}\sigma &= \frac{\pi\alpha^2}{2 M_W^2 s_\mathrm{W}^2} \frac{\mathrm{d}\phi}{2\pi} Q^2 \mathrm{d}Q^2 \frac{s^2+u^2}{2s^2}\\
&\quad \times \left(U_0 + \lambda U_\lambda + \ell \cos 2\phi\; U_\perp - \ell \sin 2\phi\; U_\psi\right),\\
U_0 &= \left(|K|^2 + |\tilde{K}|^2\right) + \lambda_V 2\mathrm{Re}\left(K\tilde{K}^*\right),\\
U_\perp &= \ell_V \left(|K|^2 - |\tilde{K}|^2\right),\\
U_\lambda &= 2\mathrm{Re}\left(K\tilde{K}^*\right) + \lambda_V \left(|K|^2 + |\tilde{K}|^2\right),\\
U_\psi &= 2\mathrm{Im}\left(K\tilde{K}^*\right). \qquad (9)
\end{aligned}
$$

With the notation of (5) it becomes evident that this equation reproduces term by term the polarization dependences of the $\gamma\gamma \to H$ process (3), in particular, $T_+, T_\parallel \to U_0$, $T_\perp \to U_\perp$, $T_- \to U_\lambda$, $T_\psi \to U_\psi$. Therefore, studies similar to the $HZ\gamma$ interaction are possible here. However, there is a difference between the effects of the linear photon polarization in these two reactions. In the $\gamma\gamma$ collisions we can control the linear polarizations and *choose* their relative orientation to study a specific contribution. In the γe collision we cannot control the relative orientation of the linear polarizations, so that some Fourier-type analysis is necessary to see the contributions of interest.

Let us now consider that there are different asymmetries. The quantities U_0 and $U_\perp$ are weakly sensitive to $\tilde{G}_Z$. The sensitivity of U_0 to the $\mathcal{CP}$ even anomalous interaction was studied, in fact, in [1,6].

The quantities U_λ and U_ψ are most sensitive to the $\mathcal{CP}$ odd anomalies. Thus, we consider the asymmetries

$$
\begin{aligned}
V_\lambda^{\mathrm{L,R}} &= \frac{\int \mathrm{d}\sigma^{\mathrm{L,R}}(\lambda) - \int \mathrm{d}\sigma^{\mathrm{L,R}}(-\lambda)}{|\lambda| \int \mathrm{d}\sigma^{\mathrm{SM}}_{\mathrm{np}}} \propto \int U_\lambda^{\mathrm{L,R}},\\
V_\psi^{\mathrm{L,R}} &= \frac{\int \mathrm{d}\sigma^{\mathrm{L,R}} \sin 2\phi}{|\ell| \int \mathrm{d}\sigma^{\mathrm{SM}}_{\mathrm{np}}} \propto \int U_\psi^{\mathrm{L,R}}, \qquad (10)
\end{aligned}
$$

with integrations spanning the region $Q^2 > Q_0^2 = 1000\,\mathrm{GeV}^2$ and the whole region of ϕ for the left-handed and right-handed polarized initial electrons. (The integrals in the denominators are calculated for the nonpolarized initial particles.) It happens that the cross sections for the left-handed polarized electrons are much higher than those for the right-handed electrons (see Fig. 5). Therefore, we present graphs for the left-handed electrons only. The anomalous effect for the right-handed electrons is also small in absolute value. We have not encountered any case where σ^{R} would be a useful source of additional information, despite that the relative value of the anomaly contribution can be higher here.

The quantity V_λ^{L} describing the helicity asymmetry is analogous to T_- in the $\gamma\gamma$ case with an accuracy of the contribution $\sim (|K|^2 + |\bar{K}|^2)$ entering with a small coefficient λ_V. This contribution results in a non-zero V_λ even in SM. Figure 6 shows the dependence of this quantity on $|g_{PZ}|$. For purposes of comparison, the effect of a $g_{P\gamma} = 0.3 \cdot 10^{-3}$ $H\gamma\gamma$ anomaly is also shown. We see that the values of this helicity asymmetry are large enough. Note that the signal/background ratio improves with the growth of energy since the SM contribution to the discussed quantity decreases approximately, $\propto \lambda_V \sim s^{-1}$, while the anomaly effect increases weakly, $\propto \ln(s/M_Z^2)$.

This figure also depicts the quantity V_ψ^{L} at different values of $|g_{PZ}|$. Again we also draw a comparison with a $H\gamma\gamma$ $\mathcal{CP}$ odd anomaly. This quantity is intrinsically smaller than V_λ^{L}, so the $\mathcal{CP}$ odd $HZ\gamma$ anomaly can be seen only at $|g_{PZ}| > 10^{-3}$.

The dependence of V_λ and V_ψ on the phase of the $HZ\gamma$ anomaly ξ_{PZ} is shown in Fig. 7. (The dependence of these quantities on the parameters of $H\gamma\gamma$ anomaly has the same form but the magnitude is somewhat larger.) These curves closely resemble the dependences of T_- and T_ψ on $\xi_{P\gamma}$ in the $\gamma\gamma \to H$ case. We see the familiar phase dependence $\propto \cos(\xi_{PZ} - \bar{\xi}_\gamma)$ or $\sin(\xi_{PZ} - \bar{\xi}_\gamma)$ (here $\bar{\xi}_i$ are the phases of G_γ and G_Z which are close to their SM values). The effect of switching on of the imaginary part of the SM contribution at $M_H \sim 160\,\mathrm{GeV}$ is clearly seen in these curves. In the phenomenological analysis, it is helpful that V_λ and V_ψ are intrinsically complementary: just as in the $\gamma\gamma \to H$ case, V_λ is the real part and V_ψ is the imaginary part of the same quantity. Therefore, at any value of M_H and ξ_{PZ} either V_λ or V_ψ will deviate strongly from the SM value.

[4] The box diagrams contribution (and their interference with other diagrams) is small in comparison with other contributions

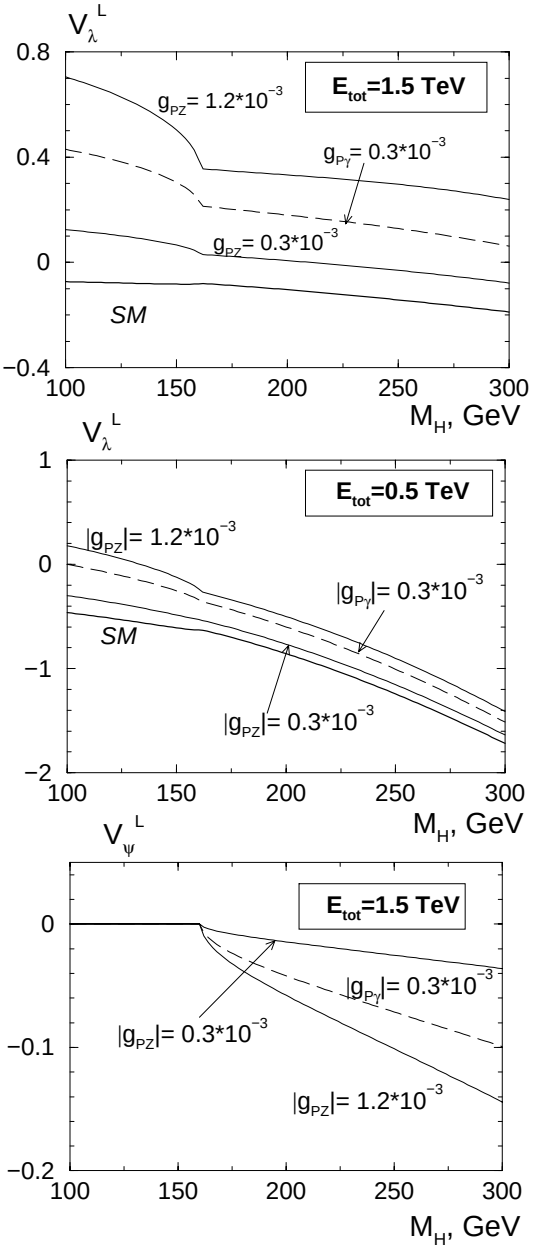

Fig. 6. The asymmetries V_λ and V_ψ; $Q^2 > 1000\,\mathrm{GeV}^2$, $\xi_{P\gamma} = \xi_{PZ} = 0$

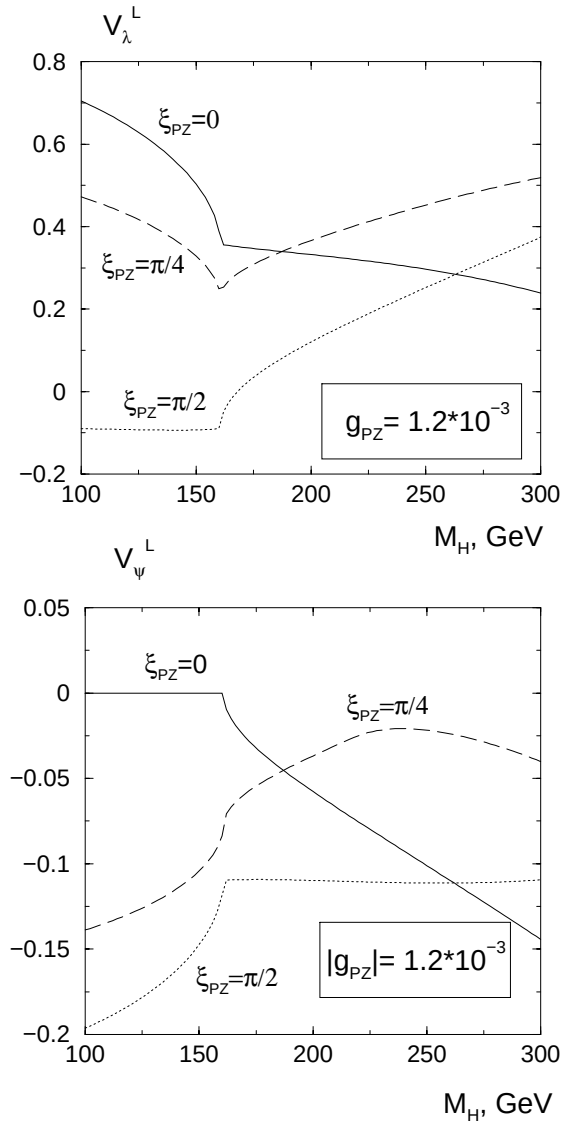

Fig. 7. The asymmetries V_λ^{L} and V_ψ at different ξ_{Pi}, $Q^2 > 1000\,\mathrm{GeV}^2$

5 Scalar–pseudoscalar mixing within the two doublet Higgs model

A specific case of $\mathcal{CP}$ violation occurs in the scalar–axial mixing within the two doublet Higgs model (2HDM). This model is described with the aid of the mixing angle β (defined via the ratio of v.e.v.'s for two basic scalar fields, $\tan\beta = \langle\phi_1\rangle/\langle\phi_2\rangle$) and three Euler mixing angles α_1, α_2, α_3 (see, for example, [21]). The observed neutral Higgs bosons are combined from the basic scalar fields by

$$\begin{pmatrix} h_1 \\ h_2 \\ h_3 \end{pmatrix} = -\sqrt{2}R \begin{pmatrix} \mathrm{Re}\phi_1^0 \\ \mathrm{Re}\phi_2^0 \\ \mathrm{Im}\left(s_\beta\phi_1^0 - c_\beta\phi_2^0\right) \end{pmatrix},$$

$$R = \begin{pmatrix} c_1 & -s_1c_2 & s_1s_2 \\ s_1c_3 & c_1c_2c_3 - s_2s_3 & -c_1s_2c_3 - c_2s_3 \\ s_1s_3 & c_1c_2s_3 + s_2c_3 & -c_1s_2s_3 + c_2c_3 \end{pmatrix}. \quad (11)$$

Here $c_i = \cos\alpha_i$, $s_i = \sin\alpha_i$. Our definition differs from that used in [21] by the minus sign in front of R in (11). The $\mathcal{CP}$ conserving case is realized at $\alpha_2 = \alpha_3 = 0$; the last angle α_1 is related to the quantity α used for the case without $\mathcal{CP}$ violation by $\alpha_1 \to \pi/2 - \alpha$, $h_1 \to h$, $h_2 \to A$, $h_3 \to -H$. Instead of α_1, below we use the angle $\delta = \beta - (\pi/2 - \alpha_1)$.

We consider only the lightest Higgs boson h_1, having in mind the decoupling regime where $M_{H^\pm}, M_{h_2}, M_{h_3} \gg M_{h_1}$. Besides, we fix the only relevant free parameter of 2HDM in the Higgs self-interaction by $\lambda_5 = 2M_{H^\pm}^2/v^2 + g^2$ (just as in the MSSM, see [22] for a definition). This choice guarantees us a negligibly small contribution of charged

Higgs loops into the discussed couplings of the Higgs boson with photons.

To describe couplings of the lightest Higgs boson h_1 with quarks and charged leptons we use the widespread "Model II" in which the ratios of these couplings to those in the minimal SM (one Higgs doublet) are

$$\begin{aligned}
\bar{u}h_1u &\to (\sin\delta + \cot\beta\cos\delta)\cos\alpha_2 \\
&\quad -\mathrm{i}\gamma^5\cot\beta\cos(\delta-\beta)\sin\alpha_2, \\
\bar{d}h_1d, \bar{\ell}h_1\ell &\to (\sin\delta - \tan\beta\cos\delta) \\
&\quad -\mathrm{i}\gamma^5\tan\beta\cos(\delta-\beta)\sin\alpha_2, \\
VVh_1 &\to \sin\delta - \sin\beta\cos(\delta-\beta)(1-\cos\alpha_2). \qquad (12)
\end{aligned}$$

The effective couplings of Higgs boson with the light G_i (1) can be written via standard loop integrals and the above mixing angles (see [1] for definitions).

$$\begin{aligned}
G^\gamma &= G^\gamma_{\mathrm{SM}}\sin\delta \\
&\quad + \frac{\alpha}{12\pi}\cos\delta\left[-\Phi_{1/2}(b)\tan\beta + 4\Phi_{1/2}(t)\cot\beta\right] \\
&\quad + \text{scalars} - \frac{\alpha}{12\pi}(1-\cos\alpha_2)\left[3\Phi_1^\gamma(W)\sin\beta\cos(\delta-\beta)\right. \\
&\quad \left. + 4\Phi_{1/2}(t)(\sin\delta + \cot\beta\cos\delta)\right], \\
\tilde{G}^\gamma &= \frac{\alpha}{12\pi}\left[\Phi^A_{1/2}(b)\tan\beta + 4\Phi^A_{1/2}(t)\cot\beta\right] \\
&\quad \times \cos(\delta-\beta)\sin\alpha_2, \\
G^Z &= G^Z_{\mathrm{SM}}\sin\delta \\
&\quad + \frac{\alpha}{4\pi}\left[v_b\Phi_{1/2}(b)\tan\beta + 2v_t\Phi_{1/2}\cot\beta\right]\cos\delta \\
&\quad + \text{scalars} - \frac{\alpha}{4\pi}(1-\cos\alpha_2)\left[\Phi_1^Z(W)\sin\beta\cos(\delta-\beta)\right. \\
&\quad \left. + 2v_t\Phi_{1/2}(t)(\sin\gamma + \cot\beta\cos\delta)\right], \\
\tilde{G}^Z &= \frac{\alpha}{4\pi}\left[2v_t\Phi^A_{1/2}(t)\cot\beta - v_b\Phi^A_{1/2}(b)\tan\beta\right] \\
&\quad \times \cos(\delta-\beta)\sin\alpha_2, \\
v_b &= -\frac{3-4s_w^2}{12s_wc_w}, \quad v_t = \frac{3-8s_w^2}{12s_wc_w}. \qquad (13)
\end{aligned}$$

The first lines in the formulas for G_γ and G_Z give their form for the standard two doublet model without $\mathcal{CP}$ mixing. At large $\tan\beta$ the imaginary part of all these couplings (arising from the b quark contribution) becomes essential. It gives phases ξ_i (2) which differ essentially from 0 or π. The corresponding values of g_i and phases ξ_i (2) could be calculated easily from these equations. The word *scalars* means the charged Higgs loop contribution; it is negligibly small in the discussed case, so we will not write it below.

Finally, all box diagrams include a VVh vertex. Therefore, the box contribution (7) to the amplitude changes by

$$B_\pm \to B_\pm^{\mathrm{SM}}\left[\sin\delta - \sin\beta\cos(\delta-\beta)(1-\cos\alpha_2)\right]. \qquad (14)$$

To make the new effects more manifest, we study the dependence on the two parameters α_2 and β only, keeping the main features of the discussed Higgs boson h_1 as close as possible to the Higgs boson of SM. For this purpose we fix the parameter $\delta \approx \pi/2$ and consider small enough values of the $\mathcal{CP}$ violating mixing angle α_2. According to (12), in this case the couplings of h with the quarks and gauge bosons are close to those in SM (see [23] for a detailed discussion of this opportunity). In this case we have instead of the previous equations

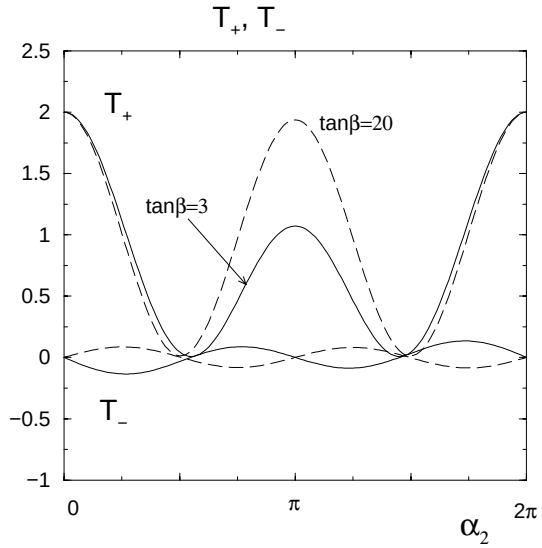

Fig. 8. Quantities $T_\pm$ in 2HDM(II), $M_h = 110\,\mathrm{GeV}$. Strong $\mathcal{CP}$ violation

$$\begin{aligned}
\bar{u}h_1u &\to \cos\alpha_2 - \mathrm{i}\gamma^5\cos\beta\sin\alpha_2, \\
\bar{d}h_1d &\to 1 - \mathrm{i}\gamma^5\tan\beta\sin\beta\sin\alpha_2, \\
VVh_1 &\to 1 - \sin^2\beta(1-\cos\alpha_2), \qquad (15)
\end{aligned}$$

$$\begin{aligned}
G^\gamma &= G^\gamma_{\mathrm{SM}} \\
&\quad - \frac{\alpha}{12\pi}(1-\cos\alpha_2)\left[3\Phi_1^\gamma(W)\sin^2\beta + 4\Phi_{1/2}(t)\right], \\
\tilde{G}^\gamma &= \frac{\alpha}{12\pi}\left[\Phi^A_{1/2}(b)\tan\beta + 4\Phi^A_{1/2}(t)\cot\beta\right]\sin\beta\sin\alpha_2, \\
G^Z &= G^Z_{\mathrm{SM}} - \frac{\alpha}{4\pi}(1-\cos\alpha_2) \\
&\quad \times \left[\Phi_1^Z(W)\sin^2\beta + 2v_t\Phi_{1/2}(t)\right], \\
\tilde{G}^Z &= \frac{\alpha}{4\pi}\left[2v_t\Phi^A_{1/2}(t)\cot\beta - v_b\Phi^A_{1/2}(b)\tan\beta\right] \\
&\quad \times \sin\beta\sin\alpha_2, \\
B_\pm &= B_\pm^{\mathrm{SM}}[1 - \sin\beta\cos\beta(1-\cos\alpha_2)]. \qquad (16)
\end{aligned}$$

Figure 8 presents the overall dependence on α_2. The strong oscillations might seem surprising. To explain them by the example of T_+, let us first note that at $\alpha_2 \approx \pi/2$ and $\tan\beta \gg 1$ the boson h_1 becomes almost pseudoscalar. Next, it is well known that the two-photon decay width of the pseudoscalar is significantly smaller than the $h \to \gamma\gamma$ decay width. Therefore, the quantity T_+ should be close to zero at $\alpha_2 \approx \pi/2$. For more details, one can consider the quantity T_+ for the case $\tan\beta = 3$, for definiteness. In this case $\sin^2\beta = 0.9$. By definition, $T_+ \propto |G|^2 + |\tilde{G}|^2$, the W contribution in the first term plays the dominant role everywhere except for a narrow region near $\alpha_2 = \pi/2$ and thus dictates the shape $T_+ \propto [1 - 0.9(1-\cos\alpha_2)]^2 +$ small remnaining terms. At α_2 slightly above $\pi/2$, when

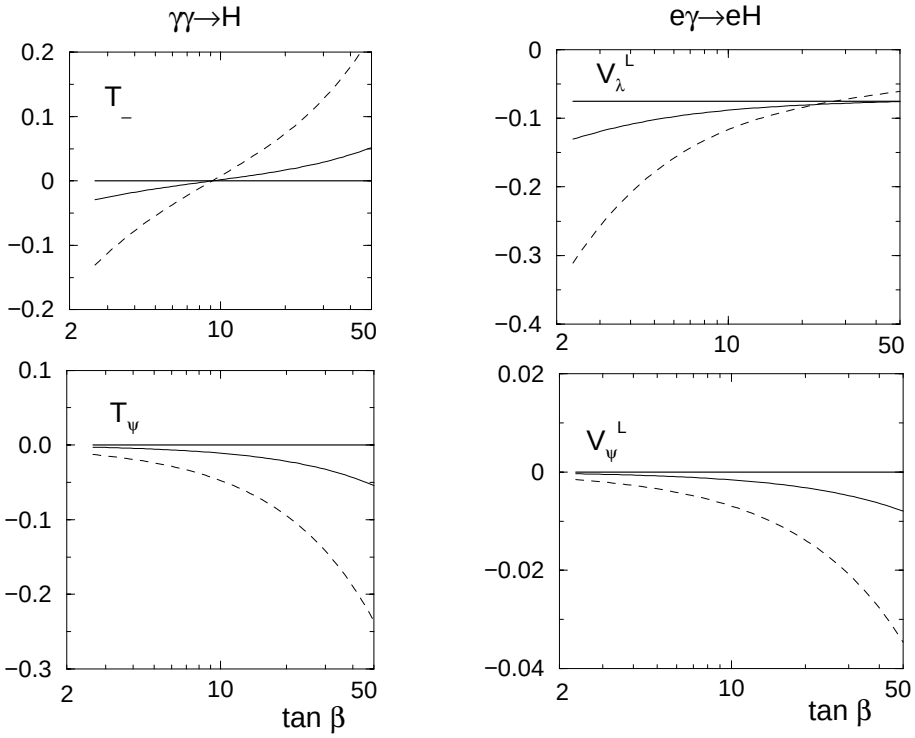

Fig. 9. Spin asymmetries in the $\gamma\gamma \to h$ and $e\gamma \to eH$ processes due to scalar–pseudoscalar mixing in 2HDM(II), $M_h = 110\,\mathrm{GeV}$; for the $e\gamma \to eH$ process $E_{\mathrm{tot}} = 1.5\,\mathrm{TeV}$. The thick solid lines show the SM values; thin solid and dashed lines refer to $\sin\alpha_2 = 0.1$ and 0.5 respectively

the t quark exactly cancels the remnant of the W boson contribution (and the real part of the b contribution), T_+ is saturated by $|\tilde{G}|^2$, which is intrinsically smaller than $|G_{\mathrm{SM}}|^2$ by two orders of magnitude. The shape of the T_- dependence on α_2 can also be foreseen from (16) in the same way. Our calculations show that the quantities $T_\perp$ and T_ψ as well as the asymmetries V_i of the $e\gamma \to eH$ reaction also exhibit a similar oscillatory dependence on α_2. The principal features of the results remain the same for other values of Higgs boson masses, including the region $M_h > 2M_W$ above the WW threshold.

However, the case of strong $\mathcal{CP}$ mixing is obviously so prominent that it will be seen at other colliders. The opposite case – the "weak mixing regime" (small values of α_2) – looks especially interesting. The above equations show that in this region $T_-, T_\psi, V_\psi \propto \alpha_2$, $V_\lambda \propto c\lambda_V + \alpha_2$, all other quantities differ from their values without $\mathcal{CP}$ mixing only a little, by a quantity $\sim \alpha_2^2$. Therefore, the asymmetries T_-, T_ψ for the $\gamma\gamma$ collisions and V_ψ, V_λ for the γe collisions are most sensitive to the weak $\mathcal{CP}$ mixing, as is seen in the figures.

The quantities T_- and T_ψ are non-zero only due to $\mathcal{CP}$ violation. Their $\tan\beta$ dependences for different α_2 are shown in Fig. 9. The measurements of both of these quantities supplement each other essentially: the asymmetry T_ψ is most sensitive to mixing effects at large $\tan\beta$, while in the small β domain the best suited quantity is T_-. This $\tan\beta$ dependence of the two quantities again can be traced to (16). The asymmetry T_-, being proportional to $\mathrm{Re}(\tilde{G}_\gamma G_\gamma^*)$, borrows its $\tan\beta$ behavior from the interplay of the b and t quark contributions to $\mathrm{Re}(\tilde{G}_\gamma)$: the b contribution, initially small, grows with $\tan\beta$. It compensates the t loop at $\tan\beta \approx 10$ and becomes dominant later on. At the same time, T_ψ has a $\tan\beta$ dependence similar to $\mathrm{Im}(\tilde{G}_\gamma)$, where we have only a b quark loop contribution. Thus, the whole asymmetry T_ψ scales as $\tan\beta$.

For the γe collisions we present only the quantities arising from $\mathcal{CP}$ non-conservation; they are $\propto \alpha_2$ at small α_2 (Fig. 9). Just as for the $\gamma\gamma$ reaction the studies of both these quantities supplement each other. The effect of a circular polarization V_λ^{L} (which is an analogue to T_-) is relatively large at $\tan\beta \sim 1$, the t/b quark loop compensation point diminishes this effect with the growth of $\tan\beta$ (it becomes zero at large $\tan\beta$). Thus, in the whole $\tan\beta$ domain under investigation the t quark loop in $\tilde{G}_i$ is dominant and therefore makes V_λ^{L} behave roughly as $\cot\beta$. On the contrary, the effect of the linear photon polarization V_ψ^{L} (which is similar to T_ψ) is very small at $\tan\beta \sim 1$ but it grows with $\tan\beta$. Nevertheless, it stays below 0.05 and thus seems hardly measurable.

The obtained results also describe the production of the lightest Higgs boson in the MSSM in the decoupling regime (when all superparticles are heavy enough). It is necessary to note in this respect that the modern calculations in the MSSM need to fix many subsidiary parameters. In the standard choice, the variation of the Higgs mass and $\tan\beta$ also shifts the quantity δ, so that the curves of [7,19], for example, present a simultaneous dependence on the parameters α_2, β and δ. That is why numerical results of [7,19] obtained for the specific problems discussed there differ from our Figs. 8 and 9. The numerical experiments show that a simple variation of the MSSM parameters A and μ allows one to have the SM-like value $\sin\delta \approx 1$ at $M_h = 105$–$125\,\mathrm{GeV}$ [23]. Our curves correspond to this very case of MSSM.

6 Discussion

In this work, together with [1], we gave detailed answers to the questions of what the whole experimentally available information about the photon–Higgs boson anomalous interactions is, and how to extract it in a reasonable way from future experiments at photon colliders. In this problem, the comparative simultaneous analysis of the two reactions $\gamma\gamma \to H$ and $e\gamma \to eH$ is useful. Due to the absence of SM couplings of the Higgs boson with photons at tree level, the signal of non-standard phenomena can appear clean in Higgs boson production in photon collisions. The high sensitivity of the reactions $\gamma\gamma \to H$ and $e\gamma \to eH$ to the admixture of various anomalous interactions makes these processes very useful in exploring the new physics beyond the TeV scale. With the new degrees of freedom of (2) in the parametric space, the unique opportunities of photon colliders in the variation of the initial photon polarization provide a new route to studying different anomalies in detail and one can be confident about a separation of the different contributions.

In our investigation we treat anomalies in a universal manner, regardless of the particular mechanism of the $\mathcal{CP}$ violation phenomenon. This is possible because, as we showed, various sources of $\mathcal{CP}$ violation are indistinguishable in the two reactions discussed having relatively large cross sections. These mechanisms are, in principle, distinguishable via the study of such processes as $\gamma\gamma \to HH$ or $\gamma\gamma \to H^* \to ZZ$ at $s \gg M_H^2$. However, they have very low cross sections and will hardly help.

Aiming at the widest class of anomalous interactions, we parameterized the amplitudes in a very general way, treating the absolute values of $|g_i|$ and the phases ξ_i of the anomalies as independent parameters. The results presented show the range of effects that could be resolved from the data; it is close to that for the $\mathcal{CP}$ even case [1]. They are $g_\gamma, g_{P\gamma} \sim 0.5 \div 1 \cdot 10^{-4}$ for the $H\gamma\gamma$ anomalies and g_Z, $g_{PZ} \sim 5 \cdot 10^{-4}$ for the $HZ\gamma$ anomalies (in terms of Λ_i introduced in [1] they read $\Lambda_\gamma, \Lambda_{P\gamma} \sim 40 \div 60\,\mathrm{TeV}$ and $\Lambda_Z, \Lambda_{PZ} \sim 20\,\mathrm{TeV}$). The effects depend strongly on the phase of the anomaly. A comparative study of the effects with circularly and linearly polarized photons is necessary to separate the effects of the amplitude and the phase of the anomaly ($|g_i|$ and ξ_i). Future simulations based on final versions of collider and detector will show the exact discovery limits before actual experiments.

Next, we analyzed some specific cases of anomalies: the presence of new particles within SM (for $\mathcal{CP}$ even anomalies [1])[5] and scalar–pseudoscalar mixing in the 2HDM. Their important feature is the definite relation among the anomalous signals in $\gamma\gamma$ and γe collisions. In particular, the study of both $\gamma\gamma$ and γe reactions is essential to test if we deal with either $\mathcal{CP}$ violating mixing in 2HDM with a definite relation among the $H\gamma\gamma$ and $HZ\gamma$ anomalies or with some other mechanism of $\mathcal{CP}$ violation with a now unpredicted relation between these two anomalies. The specific feature of the result is that signals of small mixing ($\sin\alpha_2 \sim 0.1$) are seen well in effects with a circular photon polarization at small and large $\tan\beta$ (but not at intermediate values, $\tan\beta \sim 10$), whereas the effects with linear photon polarization can be seen well at intermediate and large values of $\tan\beta$.

Lastly, it is useful to note one more advantage of an analysis of the polarization asymmetry in the production of Higgs bosons. There is a possibility in the 2HDM and MSSM that the heavier scalar Higgs boson H and its pseudoscalar counterpart A are almost degenerate within the mass resolution without $\mathcal{CP}$ violation. In this case the study of polarization asymmetries *in Higgs boson production* like those discussed above can answer the question whether $\mathcal{CP}$ is violated or not. Contrary to this, the study of asymmetries of *decay products* cannot distinguish the true $\mathcal{CP}$ violation from accidental overlapping of H and A resonance curves.

Acknowledgements. We are thankful to V. Ilyin, M. Krawczyk, V. Serbo and P. Zerwas for discussions. IPI is thankful to Prof. J. Speth for hospitality at Forschungszentrum Jülich and IFG is thankful to Prof. A. Wagner for hospitality in DESY, where the paper was finished. This work was supported by grants RFBR 99-02-17211 and 00-15-96691, grant "Universities of Russia" 015.0201.16 and grant of Sankt-Petersburg Center of fundamental studies.

[5] Note that the "existence of extra chiral generations with all fermions heavier than M_Z is strongly disfavored by the precision electroweak data. However, the data are fitted nicely even by a few extra generations, if one allows neutral leptons to have masses close to 50 GeV" [24]

References

1. A.T. Banin, I.F. Ginzburg, I.P. Ivanov, Phys. Rev. D **59**, 115001 (1999)
2. G.L. Kotkin, V.G. Serbo, Phys. Lett. B **413**, 122 (1997)
3. B. Grzadkowski, F.J. Gunion, Phys. Lett. B **294**, 361 (1992)
4. M. Kramer, J. Kuhn, M.L. Stong, P. Zerwas, Z. Phys. C **64**, 21 (1994)
5. G.J. Gounaris, F.M. Renard, Z. Phys. C **69**, 513 (1996)
6. E. Gabrielli, V.A. Ilyin, B. Mele, Phys. Rev. D **60**, 113005 (1999); Proceedings International Workshop on Linear Colliders Stiges, Spain (1999) hep-ph/9907574; hep-ph/9912321
7. S.Y. Choi, J.S. Lee, Phys. Rev. D **62**, 036005 (2000)
8. E. Asakawa, J. Kamoshita, A. Sugamoto, I. Watanabe, Eur. Phys. J. C **14**, 335 (2000)
9. I.F. Ginzburg, G.L. Kotkin, V.G. Serbo, V.I. Telnov. Pis'ma ZhETF **34**, 514 (1981); Nucl. Instr. and Meth. **205**, 47 (1983); I.F. Ginzburg, G.L. Kotkin, S.L. Panfil, V.G. Serbo, V.I. Telnov. Nucl. Instr. and Meth. **219**, 5 (1984)
10. Zeroth-order Design Report for the NLC, SLAC Report 474 (1996); R. Brinkmann et al., Nucl. Instr. and Meth. A **406**, 13 (1998); Proceedings Workshop $\gamma\gamma$ 2000, DESY, Juny, 2000, to be published
11. I.F. Ginzburg, G.L. Kotkin, Eur. Phys. J. C **13**, 295 (2000)
12. M. Melles, W.J. Stirling, V.A. Khoze, Phys. Rev. D **61**, 054015 (2000); Nucl. Phys. B (Proc. Suppl.) **82**, 379 (2000); G. Jikia, S. Söldner-Rembold, Nucl. Phys. B (Proc. Suppl.) **82**, 373 (2000)

13. B. Grzadkowski, F.J. Gunion, J. Kalinowski, Phys. Rev. D **60**, 075011 (1999)
14. M. Spira, Fortsch. Phys. **46**, 203 (1998)
15. W. Buchmuller, D. Wyler, Nucl. Phys. B **264**, 621 (1986); C.I.C. Burges, H.I. Schnitzer, Nucl. Phys. B **2**, 28 (1983) 464; C.N. Leung, S.T. Love, S. Rao, Z. Phys. C **31**, 433 (1986)
16. K. Hagiwara et al., Phys. Rev. D **48**, 2182 (1993)
17. E. Gabrielli, V.A. Ilyin, B. Mele, Phys. Rev. D **56**, 5945 (1997)
18. M. Savci, J. Phys. G **23**, 797 (1997)
19. U. Cotti, J.K. Diaz-Cruz, J.J. Toscano, Phys. Rev. D **62**, 035009 (2000)
20. V.M. Budnev, I.F. Ginzburg, G.V. Meledin, V.G. Serbo, Phys. Rep. C **15**, 181 (1975); I.F. Ginzburg, V.G. Serbo, Phys. Lett. B **103**, 68 (1981)
21. B. Grzadkowski, J.F. Gunion, J. Kalinowski, Phys. Rev. D **60**, 075011 (1999)
22. J.F. Gunion, H.E. Haber, G.L. Kane, S. Dawson, The Higgs hunter's guide (Addison–Wesley, Reading 1990)
23. I.F. Ginzburg, Nucl. Phys. B Proc. Suppl. **82**, 367 (2000); hep-ph/9907549; I.F. Ginzburg, M. Krawczyk, P. Olsen, LC note LC-TH-2000-039 (hep-ph/9909455)
24. M. Maltoni, V.A. Novikov, L.B. Okun, A.N. Rozanov, M.I. Vysotsky, Phys. Lett. B **476**, 107 (2000)